Clin Pharmacokinet (2013) 52:23–36
DOI 10.1007/s40262-012-0016-7

REVIEW ARTICLE

# Pharmacokinetics of Non-Intravenous Formulations of Fentanyl

**Jörn Lötsch · Carmen Walter · Michael J. Parnham · Bruno G. Oertel · Gerd Geisslinger**

Published online: 26 October 2012


**Abstract** Fentanyl was structurally designed by Paul Janssen in the early 1960s as a potent opioid analgesic (100-fold more potent than morphine). It is a full agonist at μ-opioid receptors and possesses physicochemical properties, in particular a high lipophilicity (octanol:water partition coefficient >700), which allow it to cross quickly between plasma and central nervous target sites (transfer half-life of 4.7–6.6 min). It undergoes first-pass metabolism via cytochrome P450 3A (bioavailability ~30 % after rapid swallowing), which can be circumvented by non-intravenous formulations (bioavailability 50–90 % for oral transmucosal or intranasal formulations). Non-intravenous preparations deliver fentanyl orally-transmucosally, intranasally or transdermally. Passive transdermal patches release fentanyl at a constant zero-order rate for 2–3 days, making them suitable for chronic pain management, as are iontophoretic transdermal systems. Oral transmucosal and intranasal routes provide fast delivery (time to reach maximum fentanyl plasma concentrations 20 min [range 20–180 min] and 12 min [range 12–21 min], respectively) suitable for rapid onset of analgesia in acute pain conditions with time to onset of analgesia of 5 or 2 min, respectively. Intranasal formulations partly bypass the blood–brain barrier and deliver a fraction of the dose directly to relevant brain target sites, providing ultra-fast analgesia for breakthrough pain. Thanks to the development of non-intravenous pharmaceutical formulations, fentanyl has become one of the most successful opioid analgesics, and can be regarded as an example of a successful reformulation strategy of an existing drug based on pharmacokinetic research and pharmaceutical technology. This development broadened the indications for fentanyl beyond the initial restriction to intra- or perioperative clinical uses. The clinical utility of fentanyl could be expanded further by more comprehensive mathematical characterizations of its parametric pharmacokinetic input functions as a basis for the rational selection of fentanyl formulations for individualized pain therapy.

J. Lötsch (✉) · C. Walter · G. Geisslinger
pharmazentrum frankfurt/ZAFES, Institute of Clinical Pharmacology, J. W. Goethe-University Hospital, Theodor-Stern-Kai 7, 60590 Frankfurt, Germany
e-mail: j.loetsch@em.uni-frankfurt.de

M. J. Parnham · B. G. Oertel
Fraunhofer IME Project Group Translational Medicine and Pharmacology (IME-TMP), Frankfurt, Germany

## 1 Introduction

Fentanyl (Fig. 1) was the first in a class of potent synthetic opioid analgesics developed in the 1960s. It is 100-fold more potent than morphine [1] and was designed by Paul Janssen [2] in a search for highly potent opioids with pronounced opioid receptor subtype specificity, which at the time was thought would improve drug safety [3]. Shortly afterwards in the 1960s, fentanyl was introduced into clinical practice as a narcotic analgesic [4]. Its use was restricted to anaesthesia until the 1990s when the development of non-injectable fentanyl formulations was intensively pursued. Elimination of the need for vessel puncturing subsequently allowed for the broader use of fentanyl as a prescriptive analgesic [5]. Nowadays, transdermal fentanyl patches are among the most frequently prescribed strong opioid analgesics [6, 7].

Fentanyl was the first opioid for which a delay between its concentration–time profile in the blood and that observed in the central nervous system (CNS) was experimentally established and mathematically modelled [8],

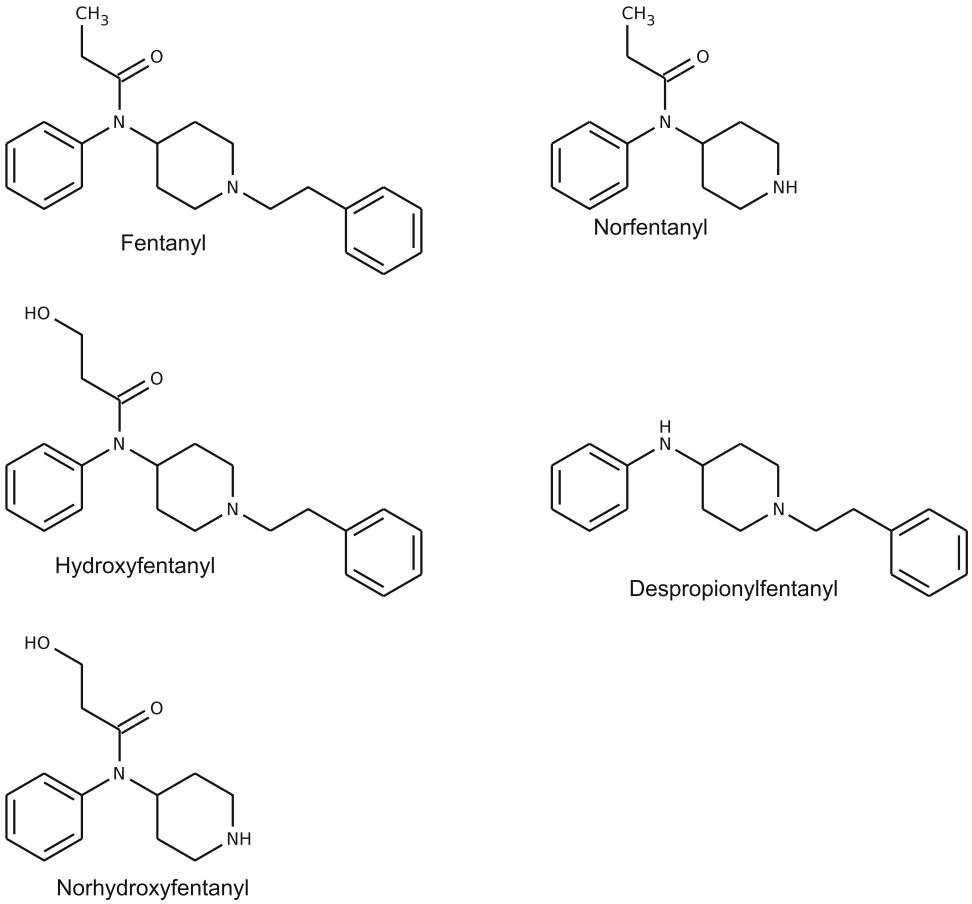


**Fig. 1** Fentanyl and its metabolites as found in an in vitro human liver microsomal system [26]. The major metabolite is norfentanyl, to which 99 % of the fentanyl is transformed. Norfentanyl is not known to produce clinically relevant pharmacodynamic effects [29]

using the relevant principles of pharmacokinetic/pharmacodynamic modelling established 7 years earlier with depolarizing neuromuscular-blocking agents [9, 10]. The development of non-injectable fentanyl formulations not only led to prolongation of the analgesic action of fentanyl, it also offered the possibility to generate a larger variety of plasma concentration–time profiles in patients in a formulation-dependent manner. This increased the therapeutic options because the clinical activity of fentanyl depends on its availability at μ-opioid receptors [11], predominantly in the CNS [12].

The different clinical indications for non-injectable fentanyl formulations, ranging from the treatment of breakthrough pain [13] with fast-acting formulations to the treatment of chronic pain with long-acting combinations, are based on the different pharmacokinetic properties of the pharmaceutical formulations. In particular, the different pharmacokinetic input characteristics of fentanyl into the central compartment, or, as in the case of nasal formulations, directly into the brain, are crucial. The key to a rational clinical use of fentanyl and all its available formulations, however, is based on the overall understanding of their pharmacokinetics, as discussed in this article.

## 2 Physicochemical and Pharmacological Properties of Fentanyl

Fentanyl represents a major success in the development of synthetic strong analgesic drugs. Subsequently developed members of the fentanyl class, such as sufentanil, carfentanil, lofentanil and alfentanil [14] or trefentanil differ from the prototype in their chemical structure mainly in the *N*-alkyl substituent of the piperidine ring (Fig. 1). In the majority of the pharmaceutical formulations currently available, fentanyl is present as the citrate salt. Besides intravenous formulations, which can also be injected intrathecally, epidurally or locally, into joints [15], fentanyl is available as transdermal patches; for nasal administration; or for oral transmucosal use as buccal lozenges, films, sublingual tablets or spray. Its physicochemical properties (Table 1), in particular its high lipophilicity (octanol:water partition coefficient >700) [16], mean that it quickly crosses between plasma and CNS effect sites with a transfer half-life ($t_{½,ke0}$), of 4.7–6.6 min [8, 17, 18].

Fentanyl exerts its actions mainly by agonist binding at μ-opioid receptors [11] (Table 1). Its pharmacological effects consist of the inhibition of the accumulation of

**Table 1** Key physicochemical and pharmacological properties of fentanyl

| Parameter | Value | References |
|---|---|---|
| Physicochemistry | | |
| Molecular weight | 336.4705 g/mol | |
| pKa | 7.89–8.6 (at 15–47.5 °C) | [113] |
| Octanol:water partition coefficient | ~717 | [16] |
| Pharmacokinetics | | |
| Protein binding | 79 % (42 % at albumin) | [114] |
| $t_{½,\beta}$ | 1.5–7 h | [25, 53] |
| $t_{½,ke0}$ | 4.7–6.6 min | [8, 17, 18] |
| $V_d$ | 60–300 L | [25] |
| F | 32 % | [53] |
| Interactions with CYP3A | Substrate and inhibitor | [26] |
| Interactions with P-glycoprotein | Substrate | [40] |
| Pharmacodynamics | | |
| $^{[3H]}$-DAMGO replacement (μ-opioid receptor affinity)[a] | 0.7 ± 0.25 nmol/L | [109] |
| $^{[3H]}$-DPDPE replacement (δ-opioid receptor affinity)[a] | 153 ± 38 nmol/L | [109] |
| $^{[3H]}$-U69,593 replacement (κ-opioid receptor affinity)[a] | 85 ± 19 nmol/L | [109] |
| $^{[3H]}$-N/OFQ replacement (orphan-opioid receptor affinity)[a] | >10,000 nmol/L | [109] |
| μ-opioid receptor cAMP inhibition | 69 ± 4 % | [110] |
| δ-opioid receptor cAMP inhibition | 71 ± 7 % | [111] |
| κ-opioid receptor cAMP inhibition | 58 ± 9 % | [112] |
| Orphan receptor $^{[35S]}$-GTPγS binding | 0.7 ± 0.25 nmol/L | [109] |

*CYP* cytochrome P450, *DAMGO* [D-Ala$^2$, N-MePhe$^4$, Gly-ol]-enkephalin, *DPDPE* [D-Pen$^2$,D-Pen$^5$]-enkephalin, *F* oral bioavailability, *GTPγS* guanosine 5′-*O*-(3-thiotriphosphate), *N/OFQ* nociceptin/orphanin FQ receptor, *pKa* acid dissociation constant, $t_{½,\beta}$ terminal plasma elimination half-life, $t_{½,ke0}$ transfer half-life between plasma and effect site, $V_d$ volume of distribution

[a] Inhibition constant values presented denote the concentration of competing ligand that would occupy 50 % of the receptors if no radioligand were present (calculated according to the Cheng–Prusoff equation)

cyclic adenosine monophosphate, presynaptic $Ca^{2+}$ influx and postsynaptic $K^+$ efflux, leading to neuronal hyperpolarization. Its clinical effects are typical for opioids, including analgesia, respiratory depression, drowsiness, nausea, vomiting and decreased gastrointestinal motility. These effects seem to be altered individually by genetic polymorphisms known to modulate opioid effects, such as the *OPRM1* variant 118A>G (rs1799971) coding for N40D μ-opioid receptors, which results in reduced expression [19] and signalling efficiency [20]. This seems to be associated occasionally [19] with a reduced analgesic response to fentanyl [21–23]. Moreover, downstream signalling components, such as potassium channels $Kir_{3.2}$, appear to act as further pharmacogenetic modulators of the pharmacodynamics of fentanyl. For instance, the genotype *KCNJ6* rs2070995 AA has been associated with increased opioid requirements, but without explicit reference to the effects of fentanyl as several other opioids were pooled in the analysis [24].

Fentanyl is extensively metabolised and renal excretion accounts for only 10 % of the dose [25]. It undergoes presystemic metabolic elimination in the liver and intestinal wall, mainly by piperidine N-dealkylation to norfentanyl (Fig. 1) as the predominant degradative pathway in humans accounting for >99 % of the metabolism [26]. In addition, it is metabolised by amide hydrolysis to despropionylfentanyl and alkyl hydroxylation to hydroxyfentanyl, the latter being further N-dealkylated to hydroxynorfentanyl [26]. This presystemic elimination reduces the bioavailability of fentanyl to 32 % [26] when it is rapidly swallowed, thus largely bypassing oral transmucosal absorption.

The metabolism of fentanyl is mediated almost exclusively by cytochrome P450 (CYP) 3A4 [26, 27] together with CYP3A5 and 3A7 [28]. The metabolites seem to lack clinically relevant opioid agonist activity [29]. The involvement of CYP3A7 contributes to a pharmacokinetic change during early development as this enzyme is the main CYP3A isoenzyme in newborns [30], but the shift to CYP3A4 dominance occurs quickly after birth [31]. However, the major consequence of the almost exclusive CYP3A-dependent metabolism is the occurrence of drug interactions. CYP3A is the main drug-metabolising enzyme [32] and fentanyl metabolism is inhibited by several inhibitors of CYP3A [33] such as ritonavir [34] or

diltiazem [35], but not by all inhibitors. Itraconazole apparently lacks influence on fentanyl metabolism [36], which can also be induced by CYP3A inducers such as phenobarbital [37]. Fentanyl may also act as an enzymatic inhibitor and reduce the clearance of co-administered drugs such as midazolam [38].

The major dependence of the fentanyl clearance on CYP3A makes it comparatively less vulnerable to genetic polymorphisms. The existence of the major *CYP3A5**3 allele, associated with reduced CYP3A5 expression and thus reduced CYP3A function [39], has been reported to cause measurable differences in the metabolism of fentanyl [28]. While the known pharmacokinetically relevant pharmacogenetic factors play a minor role in the metabolic clearance of fentanyl, clinically measurable modulation of the distribution of fentanyl seems to be produced by genetic polymorphisms in the *ABCB1* gene that encodes for P-glycoprotein (P-gp) for which fentanyl is a substrate [40]. Genotypes with lower net P-gp function, such as *ABCB1* 1236TT (rs1128503), 2677TT (rs2032582) and 3435TT (rs1045642), result in increased CNS retention of fentanyl. This is because P-gp is an outward transporter across the blood–brain barrier [41]. The compromised net P-gp function causes an increase in clinical CNS adverse effects such as respiratory depression [42, 43] and sedation [42] and reduces the need for analgesic rescue medications [44] and possibly the analgesic dosing requirements [45]. In contrast to its elimination from the CNS, the exact mechanism of the CNS uptake of fentanyl across the blood–brain barrier seems to be still unresolved and could involve passive diffusion as well as active transport by yet unspecified carriers.

## 3 Pharmaceutical Formulations for Non-Intravenous Administration of Fentanyl

For non-intravenous administration, preparations delivering fentanyl oral transmucosally, intranasally and transdermally are currently available. While transdermal patches release fentanyl in a constant sustained manner, thus being suitable for chronic pain management, the iontophoretic transdermal system and the oral transmucosal and intranasal routes of administration achieve a rapid onset of analgesia in acute pain conditions (Table 2).

## 4 Concentration–Time Profiles of Fentanyl

The actions of fentanyl are related to its concentrations at opioid receptors expressed within its main effect site, the CNS. Except for intranasal administration, whereby fentanyl is also directly delivered to the CNS [46] (Fig. 2), the extent and time course of its effects are a function of the time course of its plasma concentrations, $C_p(t)$. The profile of the latter is therefore clinically relevant and results from convolving the disposition function, $f_D(t)$, with an input function, $f_I(t)$, as in Eq. 1:

$$C_p(t) = f_I(t) * f_D(t) \quad (1)$$

where asterisk denotes convolution of the input and disposition functions.

### 4.1 Input Functions of Non-Intravenously Administered Fentanyl

The input function, $f_I(t)$, represents the major difference in fentanyl pharmacokinetic properties following various non-intravenous routes of administration because, once fentanyl has reached the blood, its disposition function, $f_D(t)$, is similar for all non-intranasal routes of administration. Depending on the clinical indication for rapid versus sustained analgesia in the therapy of breakthrough or chronic pain, respectively, pharmaceutical formulations have been developed to provide either fast or slow input functions, respectively. Unfortunately, while descriptive pharmacokinetics of non-intravenous fentanyl formulations have often been reported, including comprehensive reviews of particular formulations [47], parametric characterizations of their input functions are rare. In fact, several input functions could be used to characterize oral or oral transmucosal routes, the simplest describing a first-order input with a rate constant, $k_a$, as in Eq. 2:

$$f_{I,absorption}(t) = \text{Dose} \cdot k_a \cdot e^{-k_a \cdot t} \quad (2)$$

from which the absorption or input half-life can be calculated as $\ln(2)/k_a$.

Extravascular input of fentanyl also determines a bioavailability (F) of <1 (or <100 %), but for different reasons. Whereas incomplete absorption and pre-systemic elimination via CYP3A both reduce the bioavailability of formulations that deliver fentanyl into the gastrointestinal tract (Fig. 2), incomplete absorption of the dose from fentanyl patches, due to reduction of the concentration gradient, accounts for an F <1 with transdermal patches.

#### *4.1.1 Fentanyl Formulations for Fast Analgesic Effects*

Rapid analgesic effects are needed to cope with breakthrough pain [48], which is defined as a transitory exacerbated pain on the background of chronic pain managed with opioids [13]. It has a duration of around half an hour (range 1–240 min), is described as lancinating and has a high intensity (6–9 of an 11-point rating scale from 0 to 10) [49]. The necessary rapid analgesic onset can be achieved with oral transmucosal formulations or intranasal delivery

**Table 2** Summary of representative key descriptive pharmacokinetic parameters of non-intravenous pharmaceutical formulations of fentanyl. If available, onset and duration of analgesic effects are also given

| Parameter | Oral transmucosal | | | | | Intranasal | | Transdermal | |
|---|---|---|---|---|---|---|---|---|---|
| | Lozenge [53, 115–117, 131] | Sublingual tablet [118, 119, 132] | Sublingual spray [56, 133] | Buccal tablet [47, 120, 121, 134] | Buccal film [122, 123, 135] | Nasal spray [124, 136] | Nasal spray [71, 125, 126, 137–139] | Sustained-release patch [83, 85, 127–129, 139] | Electrotransport system [92, 93, 95, 130] |
| Product and fentanyl dosages (μg) | Actiq® (200, 400, 600, 800, 1,200, 1,600) | Abstral® (100, 200, 300, 400, 600, 800) | Subsys® (200, 400, 600, 800) | Effentora® (100, 200, 400, 600, 800) | Onsolis® (200, 400, 600, 800, 1,200) | Instanyl® (50, 200 per hub) | PecFent®, Lazanda® (100, 400 per hub) | Duragesic®, Fentadolon® (12.5, 25, 50, 75, 100 μg/h over 72 h) | Ionsys® (40 μg/dose delivered over a 10-min period, maximum amount of 3.2 mg in 24 h) |
| Bioavailability (%) | 50 | ~70 | 76 | 65 | 71 | 89 | 120, relative to Actiq® | 92 | 41 (1 h), nearly 100 % (10 h) |
| $C_{max}$ (ng/mL) | 0.39, 0.75, 1.55 and 2.51 for 200, 400, 800 and 1,600 μg, respectively | 0.24, 0.41 and 0.91 for 100, 200 and 400 μg, respectively | 0.202, 0.378, 0.8, 1.17 and 1.61 for 100, 200, 400, 600 and 800 μg, respectively | 0.24 normalized to fentanyl 100 μg | 1.33 for fentanyl 800 μg | 0.35–1.2 for fentanyl 50–200 μg | 0.351, 0.781, 1.552 and 2.844 for 100, 200, 400 and 800 μg, respectively | 1.8 for a delivery rate of 100 μg/h | 0.76–1.59 for 1.0 and 2.0 mA deliveries, respectively |
| $t_{max}$ | 23 min based on arterial blood samples | 39.7–56.7 min based on venous blood samples | 40.2–75 min[a] | 28.8 and 43.8 min for arterial and venous blood samples, respectively | 90 min based on venous blood samples | 12–15 min[a] | 15–21 min based on venous blood samples | Constant from 14 to 24 h based on venous blood samples | 122 and 119 min for 1.0 and 2.0 mA deliveries, respectively, based on venous blood samples[b] |
| $t_{½}$ | 7.6 h | 11.5–25 h | 5.25, 8.45, 11.03, 10.64 and 11.99 h for 100, 200, 400, 600 and 800 μg, respectively | 13.3 h | 19.03 h | 3–4 h | 15–24.9 h | 17 h after patch removal | 5.9–6.8 h for 1.0 and 2.0 mA deliveries, respectively |
| Onset of analgesia | 4.2 min for 200 and 800 μg | 15 min for 400 μg | 5 min | 10 min | 15 min | 2–5 min | 10 min | 12–24 h | 15 min |
| Duration of analgesia | 145 and 215 min for 200 and 800 μg, respectively | 60 min for 100–800 μg | At least 60 min | At least 60 min | At least 60 min | 120 and 240 min for 75 and 200 μg, respectively | At least 60 min | Up to 12 h after patch removal | For example, 45 min per dose of 40 μg, 24 h in total |

$C_{max}$ maximum plasma concentration, $t_{½}$ elimination half-life, $t_{max}$ time to $C_{max}$

[a] Sampling site not specified

[b] Fentanyl is detectable in plasma after 19 min, indicating the utility of iontophoretic systems for reaching analgesia quickly

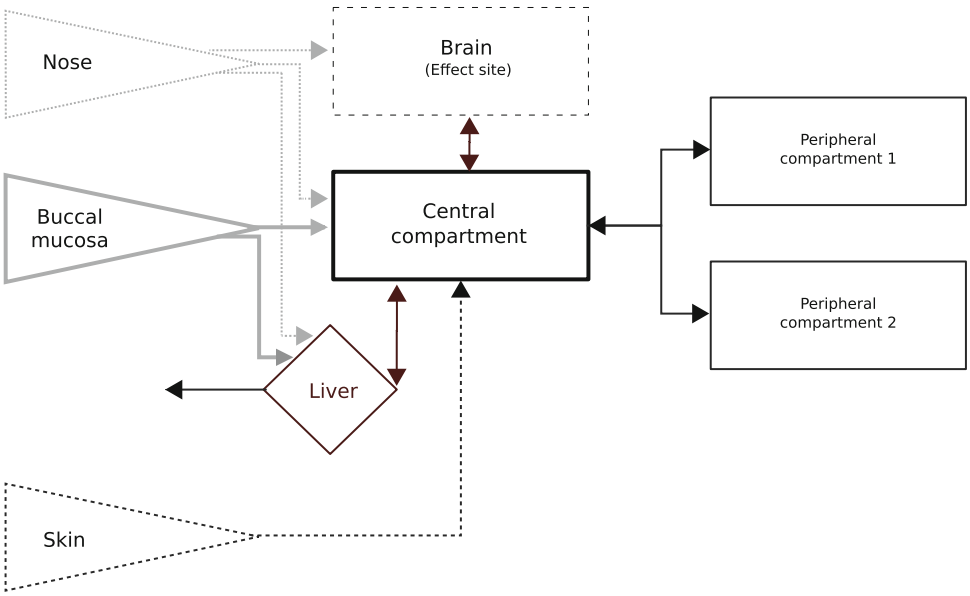


**Fig. 2** Schematic presentation of differences in the sites of fentanyl absorption in relation to different routes of non-intravenous fentanyl administration

of fentanyl. Transmucosal preparations attempt to mimic intravenous injections without vascular puncture. However, the fastest input is that given into the blood by a rapid bolus injection, which can be described by a Dirac delta function (Eq. 3) of:

$$f_{I,bolus}(t) = \text{Dose} \cdot \text{Dirac}(t) \quad (3)$$

which by definition takes a value of 1 when $t = 0$ and a value of zero otherwise, and models the input as if it were instantaneous. Fast-delivery non-intravenous fentanyl formulations attempt to draw close to this velocity of the fentanyl input.

*4.1.1.1 Oral Transmucosal Formulations* The oral route is the most accepted route of administration for drugs. However, like intravenous injections or infusions, transmucosal administration only provides rapid input into the circulation, while the time course of the effects also depends on the velocity of the transfer of fentanyl across the blood–brain barrier. As the latter is fast [8, 17, 18], oral transmucosal, either buccal or sublingual, delivery may provide the intended quick onset of analgesic effects. Hence, the pharmacokinetic profiles of fentanyl following transmucosal administration are characterized by rapid absorption. This is reflected in consistently reported short values for the time to reach the maximum (peak) plasma concentrations ($t_{max}$) after dosing, eventually supported by pharmacodynamic information on the onset and duration of analgesia (Table 2). For example, the pharmacokinetics of oral transmucosal fentanyl citrate, formulated as a sweetened lozenge on a stick and designed to dissolve slowly in the mouth, have been compared with those of a fentanyl buccal tablet formulation of transmucosal fentanyl citrate, which is manufactured to enhance the rate and extent of absorption of fentanyl [47]. Median values of $t_{max}$ were 46.8 min (range 20–240 min) and 90.8 min (range 35.0–240.1 min) for the buccal tablet and oral stick, respectively, with mean values of the maximum plasma concentration ($C_{max}$) of 1.02 ± 0.42 and 0.63 ± 0.21 ng/mL normalized to a dose of 400 µg. This is consistent with the analysis of pooled data from nine pharmacokinetic studies including a total of 365 healthy, non-opioid-tolerant adults, indicating rapid absorption from buccal tablets with $t_{max}$ ranging from 20 min to 4 h post-dose and mean values of $C_{max}$ of 0.237 ng/mL normalized to doses of 100 µg [47]. The above assessment was also used for a parametric pharmacokinetic analysis [50], but was only published as an abstract which did not give the input variables [51]. Parametric modelling of another oral transmucosal fentanyl citrate formulation utilized a first-order input, estimating a $k_a$ of 0.018 $min^{-1}$, which corresponds to an absorption half-life of 38 min [52], emphasizing that transmucosal input is slower than an intravenous injection.

The bioavailability of oral transmucosal fentanyl formulations depends on both transmucosal absorption and the absorption of the ingested dose fraction. The latter undergoes first-pass metabolism, which is bypassed by transmucosal absorption. A rapidly swallowed fentanyl solution achieved a bioavailability of 32 % [53]. A comparable value of 36 % was found in children following fentanyl lozenge application, suggesting that they swallow a considerable amount of the fentanyl [54]. Placing an oral transmucosal fentanyl unit of 15 mg/kg in the buccal pouch and sucking for 15 min raised the bioavailability to 50 % [53]. However, the input of contemporary oral transmucosal pharmaceutical preparations does not significantly

depend on the dwell time (duration of presence in the oral cavity) [47]. Despite the fact that the sublingual mucosa is thinner than the buccal mucosa, bioequivalence has been shown between sublingual and buccal placement of fentanyl preparations [55], although sublingual formulations occasionally provided higher bioavailability (Table 2) of up to 75 % of a dose [56]. Finally, mucositis occurring during cancer treatment does not seem to affect transmucosal absorption of fentanyl, at least for grade I [57], although the product information, for instance for Subsys®, warns about a four- to sevenfold higher $C_{max}$ due to mucositis.

*4.1.1.2 Intranasal Formulations* In contrast to intravenous, transdermal, subcutaneous, intramuscular, transbuccal and oral routes of administration, whereby the drug first enters the central blood compartment before crossing the blood–brain barrier to exert CNS effects, nasal routes additionally deliver the opioid directly to the CNS site of action (Fig. 2) and thus partly circumvent the blood–brain barrier [46]. Pathways that are considered likely to allow direct CNS access include the olfactory and trigeminal nerves, the vasculature, the cerebrospinal fluid and the lymphatic system [46]. The anatomy of the nose is well suited to the efficient transfer of exogenous agents into the brain [58]. This is accounted for [59] by the large surface of the nasal cavity, which is increased by the turbinates, and by the extremely high blood flow to the nasal mucosa which exceeds, relative to the tissue volume, that in muscle, brain and liver [60]. In adults, the 15–20 mL of the nasal cavity are enveloped by a surface area of 150–180 $cm^2$, 5–10 $cm^2$ of which is olfactory epithelium and the remaining 145–170 $cm^2$ is respiratory epithelium [61, 62]. In particular, the olfactory nerve seems to provide a delivery path directly into the CNS, known as the olfactory vector hypothesis [63]. Following this path, even opioids that only slowly cross the blood–brain barrier, such as morphine [64] or morphine-6-glucuronide [65], can produce rapid central nervous analgesic effects [66]. Plasma concentrations measured after intranasal fentanyl administration provide an estimate of systemic exposure and compare well with concentrations measured after intravenous injection [67]. However, local fentanyl concentrations in the CNS are probably higher after intranasal than after systemic administration due to the additional direct delivery.

The development of intranasal opioids [61] has been intensified in the last decade so that it is now possible to deliver the active compound almost instantaneously to the brain, partly bypassing the blood–brain barrier [46, 68] and reducing systemic exposure. Indeed, following intranasal administration of fentanyl 50–200 μg, the intensity difference in cancer pain at 10 min (11-point numerical rating scale from 0 to 10) was significantly better than following placebo administration, without serious adverse events, demonstrating that in opioid-tolerant patients, intranasal fentanyl is an effective treatment for breakthrough pain [69]. The bioavailability of intranasal fentanyl has been reported to be 89 % [59], perhaps due to more efficient avoidance of the oral/gastrointestinal mucosa than with transbuccal or sublingual formulations, resulting in a lower swallowed fraction of the dose. Inhaled fentanyl, by contrast, seems to be readily absorbed via the lung epithelium [70]. In order to avoid run-off through the pharynx and swallowing, the intended dose must be dissolved in a volume not more than 150 μL for intranasal administration [61], for which the high potency of fentanyl is an advantage. To enhance nasal penetration and lessen local irritation, additives such as pectin, which form a thin gel over the mucosa, have been added into newer spray formulations [71]. With this formulation, it was shown that intranasal administration provides a shorter $t_{max}$ and a higher $C_{max}$ than with oral transmucosal administration [71]. However, the pharmacokinetic parameters seemed to be comparable to other intranasal products (Table 2). Moreover, the delivery could be further enhanced by using the novel breath-actuated devices that provide significantly larger deposition in clinically important regions, possibly enhancing the delivery of drugs from the nose into the brain [72], although this technique has not yet been made available for a fentanyl formulation.

### *4.1.2 Fentanyl Formulations for Slow but Sustained Analgesic Effects*

*4.1.2.1 Passive Transdermal Therapeutic Systems* Fentanyl can be used for chronic pain treatment with continuous input from transdermal patches. The first transdermal fentanyl formulations consisted of a drug reservoir separated from the adhesive layer by a rate-limiting membrane to provide controlled drug release [73]. However, reservoir systems bore the risk of dose-dumping as a consequence of incidental leakage releasing the entire dose within a short period of time [74]. Therefore, current passive transdermal fentanyl formulations exclusively use the matrix technique with the drug dissolved in an inert polymer matrix that controls drug release [73]. This method diminishes the risk of incidental drug leakage and furthermore complicates the extraction of the drug for abuse [75]. The two delivery systems were shown to be bioequivalent, providing similar systemic concentration–time profiles and comparable tolerability [75]. Delivery results from the concentration gradient between fentanyl in the patch and the skin. Transdermal fentanyl patches constantly deliver 12.5, 25, 50, 75 or 100 μg/h over 72 h, so that a nearly zero-order delivery with a rate constant $k_0$ is technically provided. As

described previously [76], the release of fentanyl is a rate-controlled process and the amount delivered is proportional to the surface of the resorption area [77, 78]. Nevertheless, because the skin and underlying tissue need to be crossed, in contrast to delivery from the patch, the input function, $f_I(t)$, into the blood is not zero-order. Specifically, fentanyl was detected in plasma after 1–2 h, but the onset of the full analgesic effect was obtained between 12 and 24 h after patch application and may vary with local conditions such as skin temperature [79]. The mean $C_{max}$ values are proportional to the delivery rate provided by the patch, i.e. 0.3, 0.6, 1.4, 1.7 and 2.5 ng/mL, respectively, and are maintained during steady state after repeated patch applications [79].

The input function from transdermal patches has not been characterized parametrically. A pharmacokinetic/pharmacodynamic modelling approach, which was taken to overcome the difficulty in describing the release rates [80], therefore modelled the input function by cubic spline functions, akin to an earlier proposal to use linear splines [81]. A comparable technique had been used earlier to identify the absorption characteristics of a fentanyl transdermal therapeutic system delivering nominally 100 μg/h, using the Loo-Riegelman method [82] consisting of a deconvolution of the absorption function from the plasma concentration–time profiles based on the profile following intravenous administration [83]. According to this analysis, the absorption increased during the initial 4–8 h, remained relatively constant at 90.9 ± 25.7 mg/h until 24 h and subsequently decreased with a terminal absorption half-life of 16.6 ± 3.7 h.

Transdermally delivered fentanyl is not subject to first-pass metabolism (Fig. 2) and therefore provides a greater bioavailability than oral administration. However, its bioavailability from passive formulations is <1 because towards the end of the delivery interval, the concentration gradient between the transdermal therapeutic system and the skin decreases until the delivery ceases, which reduces the bioavailability of fentanyl from the patches to 92 % [84]. The absorption rate is also subject to changes in local conditions such as raised skin temperature, for instance during fever, with estimated increases in fentanyl plasma concentrations by approximately 33 % at body temperatures of 40 °C [85], with the risk of acute opioid overdose [79, 86]. In addition, in cancer patients the absorption was reported to be highly variable [87] and to depend on the patient's age, with lower absorption with higher age, and surprisingly also varied with the type of cancer, with breast or digestive cancer associated with higher absorption than lung cancer [88].

*4.1.2.2 Iontophoretic Transdermal Systems* Iontophoresis is a method for transdermal administration of ionisable drugs in which the electrically charged components are propelled through the skin by an external electric field [89]. In the fentanyl formulations, the transfer is mediated by a small electric current rather than by passive diffusion. The patch comprises a drug-containing hydrogel sandwiched between two electrodes that are arranged parallel to the skin surface, with the lower electrode attached closely to the skin via an adhesive layer [90]. No fentanyl was detected after passive (0.0 mA) fentanyl delivery, whereas with an electric current of 1–2 mA, mean times to detectable concentrations of plasma fentanyl were 33 and 19 min, respectively, and the $t_{max}$ was observed at 122 and 119 min, respectively [91]. A voltage application of 2 V for 60 s released approximately 315–340 μg of fentanyl and a single-voltage application at 16 h produced a $C_{max}$ of approximately 200 pg/mL. Consecutive voltage applications at 16 and 40 h produced a $C_{max}$ of approximately 730 pg/mL [89, 90]. Iontophoretic systems may provide both rapid onset, for example within 15 min [92], and a long duration of analgesia. In this respect, 31.9 doses (40 μg per dose) were shown to provide analgesia for 24 h, which corresponds to a mean duration of analgesia per dose of approximately 45 min [93].

As shown for the growth hormone-releasing factor and R-apomorphine, the drug delivery from iontophoretic systems can be described as a zero-order input from the patch into the skin based on a constant iontophoretic driving force with a negligible lag time for the drug to enter the skin. The release from the skin into the plasma, however, is a passive process determined by a first-order skin-release rate constant [94]. The bioavailability depends on the duration of use, achieving only 41 % in the first hour but almost 100 % after 10 h, suggesting that the increased absorption over time may be due to alterations in the electrical conductance of the skin that occur during exposure to electric current [95].

### 4.2 Plasma Disposition of Fentanyl

The disposition function can best be assessed following intravascular administration and has been parametrically modelled using differential equation systems or, more simply, as a sum of exponentials, such as in Eq. 4:

$$f_D(t) = \sum_{i=1}^{n} A_i \cdot e^{-\lambda_i} \quad (4)$$

where i denotes the number of the compartment (for fentanyl $n = 2$ or 3), A the amount of drug in the respective compartment and λ the first-order elimination rate constant from the respective compartment. Usually, arterial sampling has been employed in pharmacokinetic/pharmacodynamic assessments of fentanyl because of arteriovenous concentration differences [67]. As with

remifentanil [96], venous samples may lead to false pharmacokinetic/pharmacodynamic conclusions for fentanyl. Mean reported [8] parameter values of a three-compartment pharmacokinetic model were 0.069, 0.0059 and 0.00190 $L^{-1}$ for $\alpha_1$, $\alpha_2$ and $\alpha_3$, respectively, and those of $\lambda_1$, $\lambda_2$ and $\lambda_3$ were 0.673, 0.0370 and 0.00146 $h^{-1}$, respectively, where $\alpha$ and $\lambda$ are the coefficients and exponents of the disposition function, respectively, described as a sum of exponentials. Alternatively, the disposition of fentanyl has been described by a two-compartment model [97] parameterized as a differential equations system as follows (Eq. 5):

$$\begin{aligned} dA_1/dt &= CL \cdot C_1 - Q \cdot C_1 + Q \cdot C_2 \\ dA_2/dt &= Q \cdot C_1 - Q \cdot C_2 \end{aligned} \quad (5)$$

where the amounts of drug in a compartment are denoted by A followed by the number of the compartment (i.e. compartment 1 is the central compartment and compartment 2 is the peripheral distribution compartment); the total body clearance and the intercompartmental clearance are denoted by CL and Q, respectively, and the volumes come into play as scaling factors between concentrations (C) and amounts, i.e. $A = C \cdot V$. The numerical values from Yassen et al. [97] were CL = 0.98 L/min, Q = 3.51 L/min, $V_1$ = 19.5 L and $V_2$ = 150 L. The different volumes may also be responsible for the apparently highly variable description of the distribution volumes of fentanyl between 60 and 300 L [25]. These may depend on the pharmacokinetic models used and become inaccurate with simpler approaches such as descriptive or one-compartmental analysis and short observation times. Furthermore, the pharmacokinetics of fentanyl seem to be complicated by its possible sequestration in the lungs [98, 99], with consequences for the temporal course of its brain delivery, which has trigged the development of re-circulatory physiological pharmacokinetic models [100].

### 4.3 Concentrations at Effect Site

The effects of fentanyl can be related to its concentrations at effect site ($C_e$) using a sigmoid pharmacodynamic model [101] as in Eq. 6:

$$\text{PDmeasure} = E_0 + \frac{E_{max} \cdot C_e^{\gamma}}{EC_{50}^{\gamma} + C_e^{\gamma}} \quad (6)$$

where $E_0$ denotes the baseline value of the pharmacodynamic measure, $E_{max}$ its possible maximum and $EC_{50}$ the concentration of fentanyl at half-maximal effect. As described previously [76], plasma concentration ranges are available to which clinical effects can be associated. Thus, 50 % pain relief was achieved at concentrations of 1.35 and 1.9 ng/mL and quantified in healthy volunteers by either pain-related cortical potentials or pain intensity ratings after dental electrical stimulation, respectively [102]. To achieve clinical analgesia, fentanyl plasma concentrations between 0.3 and 1.5 ng/mL are recommended, whereas adverse effects significantly increase at concentrations >2 ng/mL [103]. The most dangerous opioid effects on respiration are reported with $EC_{50}$ values between 3.5 ± 1.4 ng/mL for respiratory rate and 6.1 ± 1.4 ng/mL for ventilatory volume [104]. The $EC_{50}$ for maximal slowing of EEG was 6.9 ± 1.5 ng/mL [18]. Although the calculations were performed on plasma concentrations, they involve steady-state considerations [105] and therefore reflect the required local CNS concentrations. However, to produce these effects, fentanyl molecules in blood must cross the blood–brain barrier. As a lipophilic compound (Table 1), fentanyl is transferred quickly with a $t_{½,ke0}$ of 6.6 min for its effects on EEG [17] and of 16.4 min for its effects on respiration [97]. The half-lives were obtained as $\ln(2)/k_{e0}$, which is the rate constant of the first-order transfer function [$f_T(t)$; Eq. 7] between plasma and a virtual effect compartment [10, 105], which for fentanyl can be assumed to represent the CNS.

$$f_T(t) = k_{e0} \cdot e^{-k_{e0} \cdot t} \quad (7)$$

The resulting short delay between the time course of fentanyl concentrations in plasma and that at the effect site is of major relevance in settings where plasma concentrations change quickly, such as following administration in fast-delivery formulations.

## 5 Future Directions

Despite the many pharmacokinetic reports on non-intravenous fentanyl preparations, mainly driven by the need for plasma concentration data for the approval of generic formulations, most are limited to descriptive pharmacokinetics such as $t_{max}$, $C_{max}$ and area under the plasma concentration–time curve. Only a few parametric assessments have been published and this incomplete knowledge on the characteristics of particular formulations impedes pharmacokinetic predictions of plasma and effect-site concentration profiles. As demonstrated 20 years ago, such information may be a valuable basis for rational opioid selection [106]. With respect to non-intravenous fentanyl, input models for sustained-release formulations are particularly lacking, and this impedes covariate associations such as the dependency of the input on age, sex, skin properties or body temperature. The occasionally used [80, 83] splines can only partially close this gap. More complex input functions provide meaningful parameters

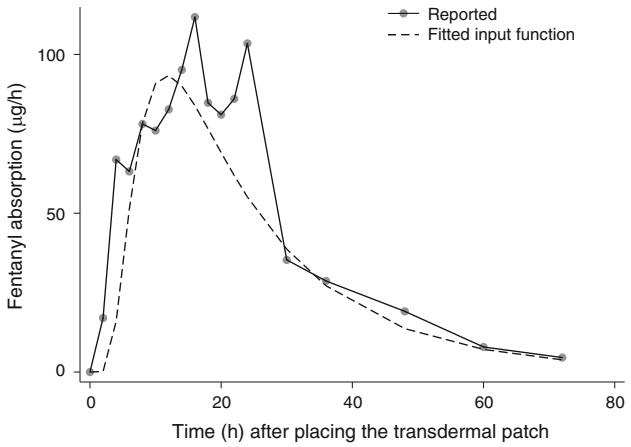


**Fig. 3** Exploratory assessment of an inverse Gaussian distribution [107] as a possible input function for transdermally delivered fentanyl. The absorption rate over time was read from a published graph (figure 5 of Varvel et al. [83]) of the input characteristics described as splines, here shown as *dots* connected by a *solid line*. Subsequently, the values of mean input time and coefficient of variation of the input function (oral bioavailability being set to a value of 1) were roughly adapted using weighted (1/y) least squares regression (Gnumeric spreadsheet solver, http://projects.gnome.org/gnumeric). This resulted in mean input time = 25.5 h and coefficient of variation = 0.76. A more exact analysis was not done as data were reconstructed from a figure without exact numerical information. It demonstrates, nevertheless, that the inverse Gaussian distribution (*dashed line*) may serve as a basis for the development of a suitable input function for transcutaneous fentanyl

for sustained-release administration, such as an inverse Gaussian distribution (Eq. 8) [107] of:

$$f_I(t) = \text{Dose} \cdot F \cdot \sqrt{\frac{MIT}{2 \cdot \pi \cdot CV_I^2 \cdot t^3}} \cdot e^{-\frac{(t-MIT)^2}{2 \cdot CV_I^2 \cdot MIT \cdot t}} \quad (8)$$

where MIT denotes the mean input time and $CV_I^2$ the normalized variance of the distribution, which provides a flexible input function [108]. This might provide a basis for a parametric input function for transdermal fentanyl administration, as exemplified in Fig. 3. Moreover, the pharmacokinetics and pharmacokinetics/pharmacodynamics of intranasal fentanyl administration have also only been addressed parametrically in an incomplete way. The model would need to take into account that the fentanyl CNS concentrations originate from direct input, bypassing the blood–brain barrier, and from input via the blood compartment.

## 6 Conclusions

From a pharmacokinetic perspective, it is the input function, $f_I(t)$, into the body by which non-intravenous formulations of fentanyl mainly differ from each other. Designed half a century ago [2], fentanyl is nowadays one of the most successful opioid analgesics [6, 7]. This success has been made possible by the pharmaceutical development of a variety of formulations, which allow non-invasive administration of fentanyl in several clinical settings of pain. These include rapid delivery from intranasal, transmucosal or transdermal iontophoretic formulations to treat breakthrough pain, in the paediatric setting for acute postoperative pain, as well as slow and partly controllable release from passive formulations with transdermal delivery for treating chronic pain. Current approaches to new drug development in the pharmaceutical industry include reformulation of previously known active substances, the development of new indications and specific patient populations, and the development of novel mechanisms of action. Among these, the development of non-intravenous formulations of fentanyl may be regarded as successful reformulation based on pharmacokinetic research, in concert with pharmaceutical technology, which expanded its use beyond the restriction to the operating [4] or recovery room. To further facilitate the clinical utility of fentanyl, parametric pharmacokinetics, in particular the mathematical characterization of input functions from the various formulations and generics, are required for the rational selection of non-intravenous fentanyl formulations for individualized pain therapy. Clinical pharmacokinetics has the necessary knowledge and tools to achieve this.

**Acknowledgments** "Landesoffensive zur Entwicklung wissenschaftlich-ökonomischer Exzellenz": "LOEWE-Schwerpunkt: Anwendungsorientierte Arzneimittelforschung" (JL and GG) for supporting the pharmacological research environment for human pharmacokinetics in a comprehensive drug development facility located at the bridge between pharmacological research in academia and in the pharmaceutical industry, hosted in the "Fraunhofer Project Group Translational Medicine and Pharmacology (IME-TMP)" at Frankfurt am Main, Germany. The authors have declared that no competing interests exist. This paper was written using Free Software programs on an office and home PC running Ubuntu GNU/Linux.

## References

1. Twycross R, Wilcock A. Palliative care formulary. 3rd ed. Oxford: palliativebooks.com; 2007. p. 269.
2. Janssen PA. A review of the chemical features associated with strong morphine-like activity. Br J Anaesth. 1962;34:260–8.
3. Stanley TH. The history and development of the fentanyl series. J Pain Symptom Manag. 1992;7(3 Suppl):S3–7.
4. Guertner T, Doenicke A, Spiess W. Neuroleptanalgesia: experiences with types I, II and their combination [in German]. Anaesthesist. 1964;13:183–9.
5. International narcotics control board: statistical information on narcotic drugs. New York: United Nations Publication; 2006.
6. NHS Information Centre. Prescription cost analysis England 2007. http://www.ic.nhs.uk/statistics-and-data-collections/primary-care/prescriptions/prescription-cost-analysis-2007. Accessed 3 Oct 2012.
7. Schwabe U, Paffrath D, editors. Arzneiverordnungs-Report 2008: Aktuelle Daten, Kosten, Trends und Kommentare. Berlin: Springer; 2008. p. 232–7.

8. Scott JC, Stanski DR. Decreased fentanyl and alfentanil dose requirements with age: a simultaneous pharmacokinetic and pharmacodynamic evaluation. J Pharmacol Exp Ther. 1987; 240(1):159–66.
9. Stanski DR, Ham J, Miller RD, Sheiner LB. Pharmacokinetics and pharmacodynamics of d-tubocurarine during nitrous oxide-narcotic and halothane anesthesia in man. Anesthesiology. 1979;51:235–41.
10. Hull CJ, Van Beem HB, McLeod K, Sibbald A, Watson MJ. A pharmacodynamic model for pancuronium. Br J Anaesth. 1978;50(11):1113–23.
11. Emmerson PJ, Liu MR, Woods JH, Medzihradsky F. Binding affinity and selectivity of opioids at mu, delta and kappa receptors in monkey brain membranes. J Pharmacol Exp Ther. 1994;271(3):1630–7.
12. Arvidsson U, Riedl M, Chakrabarti S, Lee JH, Nakano AH, Dado RJ, et al. Distribution and targeting of a mu-opioid receptor (MOR1) in brain and spinal cord. J Neurosci. 1995;15(5 Pt 1):3328–41.
13. Portenoy RK, Hagen NA. Breakthrough pain: definition, prevalence and characteristics. Pain. 1990;41:273–81.
14. Meert TF, Lu HR, van Craenndonck H, Janssen PA. Comparison between epidural fentanyl, sufentanil, carfentanil, lofentanil and alfentanil in the rat: analgesia and other in vivo effects. Eur J Anaesthesiol. 1988;5(5):313–21.
15. Uysalel A, Kecik Y, Kirdemir P, Sayin M, Binnet M. Comparison of intraarticular bupivacaine with the addition of morphine or fentanyl for analgesia after arthroscopic surgery. Arthroscopy. 1995;11(6):660–3.
16. Roy SD, Flynn GL. Solubility and related physicochemical properties of narcotic analgesics. Pharm Res. 1988;5(9):580–6.
17. Scott JC, Cooke JE, Stanski DR. Electroencephalographic quantitation of opioid effect: comparative pharmacodynamics of fentanyl and sufentanil. Anesthesiology. 1991;74(1):34–42.
18. Scott JC, Ponganis KV, Stanski DR. EEG quantitation of narcotic effect: the comparative pharmacodynamics of fentanyl and alfentanil. Anesthesiology. 1985;62:234–41.
19. Zhang Y, Wang D, Johnson AD, Papp AC, Sadée W. Allelic expression imbalance of human mu opioid receptor (OPRM1) caused by variant A118G. J Biol Chem. 2005;280(38): 32618–24.
20. Oertel BG, Kettner M, Scholich K, Renné C, Roskam B, Geisslinger G, et al. A common human micro-opioid receptor genetic variant diminishes the receptor signaling efficacy in brain regions processing the sensory information of pain. J Biol Chem. 2009;284(10):6530–5.
21. Zhang W, Chang YZ, Kan QC, Zhang LR, Lu H, Chu QJ, et al. Association of human micro-opioid receptor gene polymorphism A118G with fentanyl analgesia consumption in Chinese gynaecological patients. Anaesthesia. 2010;65(2):130–5.
22. Wu WD, Wang Y, Fang YM, Zhou HY. Polymorphism of the micro-opioid receptor gene (OPRM1 118A>G) affects fentanyl-induced analgesia during anesthesia and recovery. Mol Diagn Ther. 2009;13(5):331–7.
23. Fukuda K, Hayashida M, Ide S, Saita N, Kokita Y, Kasai S, et al. Association between OPRM1 gene polymorphisms and fentanyl sensitivity in patients undergoing painful cosmetic surgery. Pain. 2009;147(1–3):194–201.
24. Lötsch J, Prüss H, Veh RW, Doehring A. A KCNJ6 (Kir3.2, GIRK2) gene polymorphism modulates opioid effects on analgesia and addiction but not on pupil size. Pharmacogenet Genomics. 2010;20(5):291–7.
25. Mather LE. Clinical pharmacokinetics of fentanyl and its newer derivatives. Clin Pharmacokinet. 1983;8(5):422–46.
26. Labroo RB, Paine MF, Thummel KE, Kharasch ED. Fentanyl metabolism by human hepatic and intestinal cytochrome P450 3A4: implications for interindividual variability in disposition, efficacy, and drug interactions. Drug Metab Dispos. 1997;25(9): 1072–80.
27. Feierman DE, Lasker JM. Metabolism of fentanyl, a synthetic opioid analgesic, by human liver microsomes: role of CYP3A4. Drug Metab Dispos. 1996;24(9):932–9.
28. Jin M, Gock SB, Jannetto PJ, Jentzen JM, Wong SH. Pharmacogenomics as molecular autopsy for forensic toxicology: genotyping cytochrome P450 3A4*1B and 3A5*3 for 25 fentanyl cases. J Anal Toxicol. 2005;29(7):590–8.
29. Schneider E, Brune K. Opioid activity and distribution of fentanyl metabolites. Naunyn Schmiedebergs Arch Pharmacol. 1986;334(3):267–74.
30. de Wildt SN, Kearns GL, Leeder JS, van den Anker JN. Cytochrome P450 3A: ontogeny and drug disposition. Clin Pharmacokinet. 1999;37(6):485–505.
31. Lacroix D, Sonnier M, Moncion A, Cheron G, Cresteil T. Expression of CYP3A in the human liver: evidence that the shift between CYP3A7 and CYP3A4 occurs immediately after birth. Eur J Biochem. 1997;247(2):625–34.
32. Evans WE, Relling MV. Pharmacogenomics: translating functional genomics into rational therapeutics. Science. 1999; 286(5439):487–91.
33. Flockhart DA. Drug interactions: cytochrome P450 drug interaction table. Indiana University School of Medicine; 2007. http://medicine.iupui.edu/clinpharm/ddis/table.aspx. Accessed 20 Jun 2012.
34. Olkkola KT, Palkama VJ, Neuvonen PJ. Ritonavir's role in reducing fentanyl clearance and prolonging its half-life. Anesthesiology. 1999;91(3):681–5.
35. Levin TT, Bakr MH, Nikolova T. Case report: delirium due to a diltiazem-fentanyl CYP3A4 drug interaction. Gen Hosp Psychiatry. 2010;32(6):648.e9–10.
36. Palkama VJ, Neuvonen PJ, Olkkola KT. 3A4 inhibitor itraconazole has no effect on the pharmacokinetics of i.v. fentanyl. Br J Anaesth. 1998;81(4):598–600.
37. Lehmann KA, Hunger L, Brandt K, Daub D. Biotransformation of fentanyl. III: effect of chronic drug exposure on the distribution, metabolism and excretion in the rat [in German]. Der Anaesthesist. 1983;32(4):165–73.
38. Oda Y, Mizutani K, Hase I, Nakamoto T, Hamaoka N, Asada A. Fentanyl inhibits metabolism of midazolam: competitive inhibition of CYP3A4 in vitro. Br J Anaesth. 1999;82(6):900–3.
39. Kuehl P, Zhang J, Lin Y, Lamba J, Assem M, Schuetz J, et al. Sequence diversity in CYP3A promoters and characterization of the genetic basis of polymorphic CYP3A5 expression. Nat Genet. 2001;27(4):383–91.
40. Wandel C, Kim R, Wood M, Wood A. Interaction of morphine, fentanyl, sufentanil, alfentanil, and loperamide with the efflux drug transporter P-glycoprotein. Anesthesiology. 2002;96(4): 913–20.
41. de Lange EC, de Bock G, Schinkel AH, de Boer AG, Breimer DD. BBB transport and P-glycoprotein functionality using MDR1A (-/-) and wild-type mice: total brain versus microdialysis concentration profiles of rhodamine-123. Pharm Res. 1998;15(11):1657–65.
42. Kesimci E, Engin AB, Kanbak O, Karahalil B. Association between ABCB1 gene polymorphisms and fentanyl's adverse effects in Turkish patients undergoing spinal anesthesia. Gene. 2012;493(2):273–7.
43. Park HJ, Shinn HK, Ryu SH, Lee HS, Park CS, Kang JH. Genetic polymorphisms in the ABCB1 gene and the effects of fentanyl in Koreans. Clin Pharmacol Ther. 2007;81(4):539–46.
44. Takashina Y, Naito T, Mino Y, Yagi T, Ohnishi K, Kawakami J. Impact of CYP3A5 and ABCB1 gene polymorphisms on fentanyl pharmacokinetics and clinical responses in cancer patients

undergoing conversion to a transdermal system. Drug Metab Pharmacokinet (Epub 2012 Jan 24).
45. Lötsch J, von Hentig N, Freynhagen R, Griessinger N, Zimmermann M, Doehring A, et al. Cross-sectional analysis of the influence of currently known pharmacogenetic modulators on opioid therapy in outpatient pain centers. Pharmacogenet Genomics. 2009;19(6):429–36.
46. Dhuria SV, Hanson LR, Frey WH 2nd. Intranasal delivery to the central nervous system: mechanisms and experimental considerations. J Pharm Sci. 2010;99:1654–73.
47. Darwish M, Xie F. Pharmacokinetics of fentanyl buccal tablet: a pooled analysis and review. Pain Pract. 2012;12(4):307–14.
48. Smith H. A comprehensive review of rapid-onset opioids for breakthrough pain. CNS Drugs. 2012;26(6):509–35.
49. Caraceni A, Martini C, Zecca E, Portenoy RK, Ashby MA, Hawson G, et al. Breakthrough pain characteristics and syndromes in patients with cancer pain: an international survey. Palliat Med. 2004;18(3):177–83.
50. Darwish M, Hamed E, Messina J. Fentanyl buccal tablet for the treatment of breakthrough pain: pharmacokinetics of buccal mucosa delivery and clinical efficacy. Perspect Med Chem. 2010;4:11–21.
51. Kern S, Boskey J, Darwish M. Pharmacokinetics of fentanyl buccal tablet and oral transmucosal fentanyl citrate [abstract]. Anesthesiology. 2007;107:A1085.
52. Egan TD, Sharma A, Ashburn MA, Kievit J, Pace NL, Streisand JB. Multiple dose pharmacokinetics of oral transmucosal fentanyl citrate in healthy volunteers. Anesthesiology. 2000;92(3):665–73.
53. Streisand JB, Varvel JR, Stanski DR, Le Maire L, Ashburn MA, Hague BI, et al. Absorption and bioavailability of oral transmucosal fentanyl citrate. Anesthesiology. 1991;75(2):223–9.
54. Wheeler M, Birmingham PK, Dsida RM, Wang Z, Coté CJ, Avram MJ. Uptake pharmacokinetics of the Fentanyl Oralet in children scheduled for central venous access removal: implications for the timing of initiating painful procedures. Paediatr Anaesth. 2002;12(7):594–9.
55. Paech MJ, Bloor M, Schug SA. New formulations of fentanyl for acute pain management. Drugs Today (Barc). 2012;48(2):119–32.
56. Rauck R, Reynolds L, Geach J, Bull J, Stearns L, Scherlis M, et al. Efficacy and safety of fentanyl sublingual spray for the treatment of breakthrough cancer pain: a randomized, double-blind, placebo-controlled study. Curr Med Res Opin. 2012;28:859–70.
57. Finn AL, Hill WC, Tagarro I, Gever LN. Absorption and tolerability of fentanyl buccal soluble film (FBSF) in patients with cancer in the presence of oral mucositis. J Pain Res. 2011;4:245–51.
58. Doty RL. The olfactory vector hypothesis of neurodegenerative disease: is it viable? Ann Neurol. 2008;63:7–15.
59. Panagiotou I, Mystakidou K. Intranasal fentanyl: from pharmacokinetics and bioavailability to current treatment applications. Expert Rev Anticancer Ther. 2010;10(7):1009–21.
60. Bende M, Flisberg K, Larsson I, Ohlin P, Olsson P. A method for determination of blood flow with 133Xe in human nasal mucosa. Acta Otolaryngol. 1983;96(3–4):277–85.
61. Dale O, Hjortkjaer R, Kharasch ED. Nasal administration of opioids for pain management in adults. Acta Anaesthesiol Scand. 2002;46:759–70.
62. Peng PW, Sandler AN. A review of the use of fentanyl analgesia in the management of acute pain in adults. Anesthesiology. 1999;90(2):576–99.
63. Prediger RDS, Aguiar AS, Matheus FC, Walz R, Antoury L, Raisman-Vozari R, et al. Intranasal administration of neurotoxicants in animals: support for the olfactory vector hypothesis of Parkinson's disease. Neurotox Res. 2012;21(1):90–116.
64. Skarke C, Darimont J, Schmidt H, Geisslinger G, Lötsch J. Analgesic effects of morphine and morphine-6-glucuronide in a transcutaneous electrical pain model in healthy volunteers. Clin Pharmacol Ther. 2003;73(1):107–21.
65. Lötsch J, Skarke C, Schmidt H, Grösch S, Geisslinger G. The transfer half-life of morphine-6-beta-glucuronide from plasma to effect site assessed by pupil size measurement in healthy volunteers. Anesthesiology. 2001;95(6):1329–38.
66. Illum L, Davis SS, Pawula M, Fisher AN, Barrett DA, Farraj NF, et al. Nasal administration of morphine-6-glucuronide in sheep: a pharmacokinetic study. Biopharm Drug Dispos. 1996;17:717–24.
67. Moksnes K, Fredheim OM, Klepstad P, Kaasa S, Angelsen A, Nilsen T, et al. Early pharmacokinetics of nasal fentanyl: is there a significant arterio-venous difference? Eur J Clin Pharmacol. 2008;64(5):497–502.
68. Graff CL, Pollack GM. Nasal drug administration: potential for targeted central nervous system delivery. J Pharm Sci. 2005;94:1187–95.
69. Kress HG, Orońska A, Kaczmarek Z, Kaasa S, Colberg T, Nolte T. Efficacy and tolerability of intranasal fentanyl spray 50 to 200 microg for breakthrough pain in patients with cancer: a phase III, multinational, randomized, double-blind, placebo-controlled, crossover trial with a 10-month, open-label extension treatment. Clin Ther. 2009;31(6):1177–91.
70. Waters CM, Krejcie TC, Avram MJ. Facilitated uptake of fentanyl, but not alfentanil, by human pulmonary endothelial cells. Anesthesiology. 2000;93(3):825–31.
71. Fisher A, Watling M, Smith A, Knight A. Pharmacokinetics and relative bioavailability of fentanyl pectin nasal spray 100–800 μg in healthy volunteers. Int J Clin Pharmacol Ther. 2010;48(12):860–7.
72. Djupesland PG, Skretting A, Winderen M, Holand T. Breath actuated device improves delivery to target sites beyond the nasal valve. Laryngoscope. 2006;116(3):466–72.
73. Prodduturi S, Sadrieh N, Wokovich AM, Doub WH, Westenberger BJ, Buhse L. Transdermal delivery of fentanyl from matrix and reservoir systems: effect of heat and compromised skin. J Pharm Sci. 2010;99(5):2357–66.
74. Forsgren J, Jämstorp E, Bredenberg S, Engqvist H, Strømme M. A ceramic drug delivery vehicle for oral administration of highly potent opioids. J Pharm Sci. 2010;99(1):219–26.
75. Marier JF, Lor M, Potvin D, Dimarco M, Morelli G, Saedder EA. Pharmacokinetics, tolerability, and performance of a novel matrix transdermal delivery system of fentanyl relative to the commercially available reservoir formulation in healthy subjects. J Clin Pharmacol. 2006;46(6):642–53.
76. Walter C, Felden L, Lötsch J. Bioequivalence criteria for transdermal fentanyl generics: do these need a relook? Clin Pharmacokinet. 2009;48(10):625–33.
77. Koehntop DE, Rodman JH. Fentanyl pharmacokinetics in patients undergoing renal transplantation. Pharmacotherapy. 1997;17:746–52.
78. Haberer JP, Schoeffler P, Couderc E, Duvaldestin P. Fentanyl pharmacokinetics in anaesthetized patients with cirrhosis. Br J Anaesth. 1982;54:1267–70.
79. Newshan G. Heat-related toxicity with the fentanyl transdermal patch. J Pain Symptom Manag. 1998;16(5):277–8.
80. Andresen T, Upton RN, Foster DJR, Christrup LL, Arendt-Nielsen L, Drewes AM. Pharmacokinetic/pharmacodynamic relationships of transdermal buprenorphine and fentanyl in experimental human pain models. Basic Clin Pharmacol Toxicol. 2011;108(4):274–84.
81. Unadkat JD, Bartha F, Sheiner LB. Simultaneous modeling of pharmacokinetics and pharmacodynamics with nonparametric kinetic and dynamic models. Clin Pharmacol Ther. 1986;40(1):86–93.

82. Loo JC, Riegelman S. New method for calculating the intrinsic absorption rate of drugs. J Pharm Sci. 1968;57(6):918–28.
83. Varvel JR, Shafer SL, Hwang SS, Coen PA, Stanski DR. Absorption characteristics of transdermally administered fentanyl. Anesthesiology. 1989;70(6):928–34.
84. Bentley JB, Borel JD, Nenad RE Jr, Gillespie TJ. Age and fentanyl pharmacokinetics. Anesth Analg. 1982;61(12):968–71.
85. Janssen Pharmaceuticals, Inc. Duragesic: Full prescribing information. Titusville: Janssen Pharmaceuticals, Inc.; 2011.
86. Carter KA. Heat-associated increase in transdermal fentanyl absorption. Am J Health Syst Pharm. 2003;60(2):191–2.
87. Solassol I, Bressolle F, Caumette L, Garcia F, Poujol S, Culine S, et al. Inter- and intraindividual variabilities in pharmacokinetics of fentanyl after repeated 72-hour transdermal applications in cancer pain patients. Ther Drug Monit. 2005;27(4):491–8.
88. Solassol I, Caumette L, Bressolle F, Garcia F, Thézenas S, Astre C, et al. Inter- and intra-individual variability in transdermal fentanyl absorption in cancer pain patients. Oncol Rep. 2005;14(4):1029–36.
89. Schröder B, Nickel U, Meyer E, Lee G. Transdermal delivery using a novel electrochemical device, part 2: in vivo study in humans. J Pharm Sci. 2012;101(6):2262–8.
90. Schröder B, Nickel U, Meyer E, Lee G. Transdermal delivery using a novel electrochemical device, part 1: device design and in vitro release/permeation of fentanyl. J Pharm Sci. 2012;101(1):245–55.
91. Ashburn MA, Streisand J, Zhang J, Love G, Rowin M, Niu S, et al. The iontophoresis of fentanyl citrate in humans. Anesthesiology. 1995;82(5):1146–53.
92. Panchal SJ, Damaraju CV, Nelson WW, Hewitt DJ, Schein JR. System-related events and analgesic gaps during postoperative pain management with the fentanyl iontophoretic transdermal system and morphine intravenous patient-controlled analgesia. Anesth Analg. 2007;105(5):1437–41.
93. Viscusi ER, Siccardi M, Damaraju CV, Hewitt DJ, Kershaw P. The safety and efficacy of fentanyl iontophoretic transdermal system compared with morphine intravenous patient-controlled analgesia for postoperative pain management: an analysis of pooled data from three randomized, active-controlled clinical studies. Anesth Analg. 2007;105(5):1428–36.
94. Nugroho AK, Della-Pasqua O, Danhof M, Bouwstra JA. Compartmental modeling of transdermal iontophoretic transport II: in vivo model derivation and application. Pharm Res. 2005;22(3):335–46.
95. Sathyan G, Jaskowiak J, Evashenk M, Gupta S. Characterisation of the pharmacokinetics of the fentanyl HCl patient-controlled transdermal system (PCTS): effect of current magnitude and multiple-day dosing and comparison with IV fentanyl administration. Clin Pharmacokinet. 2005;44(Suppl 1):7–15.
96. Hermann DJ, Egan TD, Muir KT. Influence of arteriovenous sampling on remifentanil pharmacokinetics and pharmacodynamics. Clin Pharmacol Ther. 1999;65(5):511–8.
97. Yassen A, Olofsen E, Romberg R, Sarton E, Teppema L, Danhof M, et al. Mechanism-based PK/PD modeling of the respiratory depressant effect of buprenorphine and fentanyl in healthy volunteers. Clin Pharmacol Ther. 2006/12/23 ed. 2007;81(1):50–8.
98. Taeger K, Weninger E, Schmelzer F, Adt M, Franke N, Peter K. Pulmonary kinetics of fentanyl and alfentanil in surgical patients. Br J Anaesth. 1988;61(4):425–34.
99. Bentley JB, Conahan TJ, Cork RC. Fentanyl sequestration in lungs during cardiopulmonary bypass. Clin Pharmacol Ther. 1983;34(5):703–6.
100. Upton RN, Grant C, Martinez AM, Ludbrook GL. Recirculatory model of fentanyl disposition with the brain as the target organ. Br J Anaesth. 2004;93(5):687–97.
101. Holford NH, Sheiner LB. Kinetics of pharmacologic response. Pharmacol Ther. 1982;16(2):143–66.
102. Hill HF, Chapman CR, Saeger LS, Bjurstrom R, Walter MH, Schoene RB, et al. Steady-state infusions of opioids in human. II. Concentration-effect relationships and therapeutic margins. Pain. 1990;43:69–79.
103. GmbH Janssen-Cilag. Durogesic SMAT: Fachinformation (Stand: 2011). Neuss: Janssen-Cilag GmbH; 2011.
104. Mildh LH, Scheinin H, Kirvela OA. The concentration-effect relationship of the respiratory depressant effects of alfentanil and fentanyl. Anesth Analg. 2001;93(4):939–46.
105. Sheiner LB, Stanski DR, Vozeh S, Miller RD, Ham J. Simultaneous modeling of pharmacokinetics and pharmacodynamics: application to d-tubocurarine. Clin Pharmacol Ther. 1979;25:358–71.
106. Shafer SL, Varvel JR. Pharmacokinetics, pharmacodynamics, and rational opioid selection. Anesthesiology. 1991;74:53–63.
107. Wang J, Weiss M, D'Argenio DZ. A note on population analysis of dissolution-absorption models using the inverse Gaussian function. J Clin Pharmacol. 2008;48(6):719–25.
108. Lötsch J, Weiss M, Ahne G, Kobal G, Geisslinger G. Pharmacokinetic modeling of M6G formation after oral administration of morphine in healthy volunteers. Anesthesiology. 1999;90(4):1026–38.
109. Zaveri N, Polgar WE, Olsen CM, Kelson AB, Grundt P, Lewis JW, et al. Characterization of opiates, neuroleptics, and synthetic analogs at ORL1 and opioid receptors. Eur J Pharmacol. 2001;428(1):29–36.
110. Gharagozlou P, Demirci H, David Clark J, Lameh J. Activity of opioid ligands in cells expressing cloned mu opioid receptors. BMC Pharmacol. 2003 Jan 4;3:1.
111. Gharagozlou P, Demirci H, Clark JD, Lameh J. Activation profiles of opioid ligands in HEK cells expressing delta opioid receptors. BMC Neurosci. 2002;18(3):19.
112. Gharagozlou P, Hashemi E, DeLorey TM, Clark JD, Lameh J. Pharmacological profiles of opioid ligands at kappa opioid receptors. BMC Pharmacol. 2006;6:3.
113. Thurlkill RL, Cross DA, Scholtz JM, Pace CN. pKa of fentanyl varies with temperature: implications for acid-base management during extremes of body temperature. J Cardiothorac Vasc Anesth. 2005;19(6):759–62.
114. Bower S. Plasma protein binding of fentanyl. J Pharm Pharmacol. 1981;33(8):507–14.
115. Mystakidou K, Katsouda E, Parpa E, Vlahos L, Tsiatas ML. Oral transmucosal fentanyl citrate: overview of pharmacological and clinical characteristics. Drug Deliv. 2006;13:269–76.
116. Darwish M, Tempero K, Kirby M, Thompson J. Relative bioavailability of the fentanyl effervescent buccal tablet (FEBT) 1,080 pg versus oral transmucosal fentanyl citrate 1,600 pg and dose proportionality of FEBT 270 to 1,300 microg: a single-dose, randomized, open-label, three-period study in healthy adult volunteers. Clin Ther. 2006;28(5):715–24.
117. Lichtor JL, Sevarino FB, Joshi GP, Busch MA, Nordbrock E, Ginsberg B. The relative potency of oral transmucosal fentanyl citrate compared with intravenous morphine in the treatment of moderate to severe postoperative pain. Anesth Analg. 1999;89:732–8.
118. Lennernäs B, Hedner T, Holmberg M, Bredenberg S, Nyström C, Lennernäs H. Pharmacokinetics and tolerability of different doses of fentanyl following sublingual administration of a rapidly dissolving tablet to cancer patients: a new approach to treatment of incident pain. Br J Clin Pharmacol. 2005;59:249–53.
119. Chwieduk CM, McKeage K. Fentanyl sublingual: in breakthrough pain in opioid-tolerant adults with cancer. Drugs. 2010;70:2281–8.

120. Darwish M, Kirby M, Robertson P, Hellriegel E, Jiang JG. Comparison of equivalent doses of fentanyl buccal tablets and arteriovenous differences in fentanyl pharmacokinetics. Clin Pharmacokinet. 2006;45(8):843–50.
121. Portenoy RK, Messina J, Xie F, Peppin J. Fentanyl buccal tablet (FBT) for relief of breakthrough pain in opioid-treated patients with chronic low back pain: a randomized, placebo-controlled study. Curr Med Res Opin. 2007;23:223–33.
122. Rauck R, North J, Gever LN, Tagarro I, Finn ALC-2875549. Fentanyl buccal soluble film (FBSF) for breakthrough pain in patients with cancer: a randomized, double-blind, placebo-controlled study. Ann Oncol. 2010;21:1308–14.
123. Vasisht N, Gever LN, Tagarro I, Finn AL. Single-dose pharmacokinetics of fentanyl buccal soluble film. Pain Med. 2010;11(7):1017–23.
124. Foster D, Upton R, Christrup L, Popper L. Pharmacokinetics and pharmacodynamics of intranasal versus intravenous fentanyl in patients with pain after oral surgery. Ann Pharmacother. 2008;42:1380–7.
125. Curtiss CP. Fentanyl pectin nasal spray reduces breakthrough cancer pain intensity compared with placebo in people taking at least 60 mg daily oral morphine or equivalent. Evid Based Nurs. 2011;14:90–1.
126. Watts P, Smith A. PecSys: in situ gelling system for optimised nasal drug delivery. Expert Opin Drug Deliv. 2009;6:543–52.
127. Sandler A. Transdermal fentanyl: acute analgesic clinical studies. J Pain Symptom Manag. 1992;7:S27–35.
128. Gourlay GK, Kowalski SR, Plummer JL, Cherry DA, Szekely SM, Mather LE, et al. The efficacy of transdermal fentanyl in the treatment of postoperative pain: a double-blind comparison of fentanyl and placebo systems. Pain. 1990;40:21–8.
129. Severino FB, Paige D, Sinatra RS, Silverman DG. Postoperative analgesia with parenteral opioids: does continuous delivery utilizing a transdermal opioid preparation affect analgesic efficacy or patient safety? J Clin Anesth. 1997;9(3):173–8.
130. Ashburn MA, Ogden LL, Zhang J, Love G, Basta SV. The pharmacokinetics of transdermal fentanyl delivered with and without controlled heat. J Pain. 2003;4(6):291–7.
131. Cephalon, Inc. Actiq: full prescribing information. Frazer: Cephalon Inc.; 2011.
132. ProStrakan Ltd. Abstral: summary of product characteristics. Galashiels: ProStrakan Ltd; 2010.
133. Insys Therapeutics, Inc. Subsys: full prescribing information. Phoenix: Insys Therapeutics, Inc.; 2012.
134. Cephalon Europe. Effentora: fachinformation. Maisons-Alfort: Cephalon Europe; 2011.
135. Meda Pharmaceuticals, Inc. Onsolis: full prescribing information. Somerset: Meda Pharmaceuticals, Inc.; 2011.
136. Nycomed Danmark ApS. Instanyl: fachinformation. Roskile: Nycomed Danmark ApS; 2011.
137. Archimedes Pharma Germany GmbH. PecFent: fachinformation. Mannheim: Archimedes Pharma Germany GmbH; 2010.
138. Archimedes Pharma US, Inc. Lazanda: full prescribing information. Reading: Archimedes Pharma Ltd; 2012.
139. Mibe GmbH Arzneimittel. Fentadolon: Fachinformation. Brehna: Mibe GmbH Arzneimittel; 2010.